

Measurement of the D_s Lifetime

Fermilab E791 Collaboration

E. M. Aitala,ⁱ S. Amato,^a J. C. Anjos,^a J. A. Appel,^e
D. Ashery,ⁿ S. Banerjee,^e I. Bediaga,^a G. Blaylock,^h
S. B. Bracker,^o P. R. Burchat,^m R. A. Burnstein,^f T. Carter,^e
H. S. Carvalho,^a N. K. Coptly,^l L. M. Cremaldi,ⁱ C. Darling,^r
K. Denisenko,^e A. Fernandez,^k G. F. Fox,^l P. Gagnon,^b
C. Gobel,^a K. Gounder,ⁱ A. M. Halling,^e G. Herrera,^d
G. Hurvits,ⁿ C. James,^e P. A. Kasper,^f S. Kwan,^e
D. C. Langs,^l J. Leslie,^b B. Lundberg,^e S. Maytal-Beck,ⁿ
B. Meadows,^c J. R. T. de Mello Neto,^a D. Mihalcea,^g
R. H. Milburn,^p J. M. de Miranda,^a A. Napier,^p A. Nguyen,^g
A. B. d'Oliveira,^{c,k} K. O'Shaughnessy,^b K. C. Peng,^f
L. P. Perera,^c M. V. Purohit,^l B. Quinn,ⁱ S. Radeztsky,^q
A. Rafatian,ⁱ N. W. Reay,^g J. J. Reidy,ⁱ A. C. dos Reis,^a
H. A. Rubin,^f D. A. Sanders,ⁱ A. K. S. Santha,^c
A. F. S. Santoro,^a A. J. Schwartz,^c M. Sheaff,^{d,q}
R. A. Sidwell,^g A. J. Slaughter,^r M. D. Sokoloff,^c J. Solano,^a
N. R. Stanton,^g R. J. Stefanski,^e K. Stenson,^q D. J. Summers,ⁱ
S. Takach,^r K. Thorne,^e A. K. Tripathi,^g S. Watanabe,^q
R. Weiss-Babai,ⁿ J. Wiener,^j N. Witchey,^g E. Wolin,^r
S. M. Yang,^g D. Yi,ⁱ S. Yoshida,^g R. Zaliznyak,^m
and C. Zhang^g

^a*Centro Brasileiro de Pesquisas Físicas, Rio de Janeiro RJ, Brazil*

^b*University of California, Santa Cruz, California 95064*

^c*University of Cincinnati, Cincinnati, Ohio 45221*

^d*CINVESTAV, 07000 Mexico City, DF Mexico*

^e*Fermilab, Batavia, Illinois 60510*

^f*Illinois Institute of Technology, Chicago, Illinois 60616*

^g*Kansas State University, Manhattan, Kansas 66506*

^h*University of Massachusetts, Amherst, Massachusetts 01003*

ⁱ*University of Mississippi, University, Mississippi 38677*

^j*Princeton University, Princeton, New Jersey 08544*

^k*Universidad Autonoma de Puebla, Puebla, Mexico*

^l*University of South Carolina, Columbia, South Carolina 29208*

^m*Stanford University, Stanford, California 94305*

ⁿ*Tel Aviv University, Tel Aviv, 69978 Israel*

^o*Box 1290, Enderby, British Columbia, V0E 1V0, Canada*

^p*Tufts University, Medford, Massachusetts 02155*

^q*University of Wisconsin, Madison, Wisconsin 53706*

^r*Yale University, New Haven, Connecticut 06511*

Abstract

We report the results of a precise measurement of the D_s meson lifetime based on 1662 ± 56 fully reconstructed $D_s \rightarrow \phi\pi$ decays, from the charm hadroproduction experiment E791 at Fermilab. Using an unbinned maximum likelihood fit, we measure the D_s lifetime to be $0.518 \pm 0.014 \pm 0.007$ ps. The ratio of the measured D_s lifetime to the world average D^0 lifetime [1] is 1.25 ± 0.04 . This result differs from unity by six standard deviations, indicating significantly different lifetimes for the D_s and the D^0 .

PACS: 13.25.Ft, 14.40.Lb

Precise measurements of the lifetimes of the weakly decaying charm mesons are useful for understanding the contributions of various weak decay mechanisms. Despite the fact that they are all tied to the charm quark decay, the decays of the ground-state charm mesons can have different contributions from the four first-order processes (two spectator, W-annihilation, and W-exchange), and the lifetimes are, in fact, quite different [1]:

$$\tau(D^+) : \tau(D^0) : \tau(D_s) = 2.5 : 1 : 1.1$$

The least well measured among these lifetimes is that of the D_s , which is known only to about the 4% level [2]. It is clear that there is a very large difference between the lifetime of the D^+ and that of the D^0 or D_s . However, the current measurements are only suggestive of a difference between the lifetimes of the D^0 and the D_s :

$$\frac{\tau(D_s)}{\tau(D^0)} = 1.13 \pm 0.04 \quad (3\sigma \text{ difference from unity}).$$

A more precise measurement of the lifetime of the D_s could more clearly

establish whether the lifetimes of the D^0 and D_s are indeed different.

The large difference between the D^+ and D^0 lifetimes might be explained by a large contribution from W-exchange in D^0 decays and/or large destructive interference between D^+ decay amplitudes. A difference between the D^0 and D_s lifetimes could be due to phase space differences, color factors, W-exchange, W-annihilation, decay via τ lepton modes, or relativistic effects [3,4]. The sensitivity of the D^0 - D_s lifetime difference to W-annihilation is noted in the paper by Bigi *et al.* [4]. However, spectator decays of the D_s have one more strange quark than spectator decays of the D^0 ; hence, the Cabibbo-favored hadronic final states have an extra kaon and correspondingly smaller phase space. Table 1 compares the phase space available for 2, 3, 4, and 5-body decays of the two mesons. The table shows that phase space differences alone could account for the currently observed lifetime differences.

In this letter, we report results of a high-statistics measurement of the D_s lifetime based on data from the charm hadroproduction experiment E791 at Fermilab. (Unless otherwise specified, charge conjugate states are implicitly included in this letter.) This measurement establishes more certainly a difference between the lifetimes of the D^0 and the D_s . We use only the decay mode $D_s \rightarrow \phi\pi$ since the ϕ mass constraint gives a D_s sample with a very good signal-to-noise ratio. The reconstruction efficiency as a function of lifetime was determined from data for the Cabibbo-favored (CF) decay $D^+ \rightarrow K^-\pi^+\pi^+$ and from the ratio of the efficiency for $D_s \rightarrow \phi\pi$ to that for $D^+ \rightarrow K^-\pi^+\pi^+$ obtained from Monte Carlo (MC) simulations. With this technique, most uncertainties that arise from MC simulation should cancel.

E791 [5] is a high statistics charm experiment which acquired data at Fermilab during the 1991-1992 fixed-target run. The experiment combined a fast data acquisition system with an open trigger. Over 2×10^{10} events were collected with the Tagged Photon Spectrometer using a 500 GeV π^- beam. There were five target foils with 15 mm center-to-center separations: one 0.5 mm thick platinum foil followed by four 1.6 mm thick diamond foils. The spectrometer included 23 planes of silicon microstrip detectors (6 upstream and 17 downstream of the target), 2 dipole magnets, 10 planes of proportional wire chambers (8 upstream and 2 downstream of the target), 35 drift chamber planes, 2 multi-cell threshold Čerenkov counters that provided π/K separation in the 6–60 GeV/ c momentum range [6], electromagnetic and hadronic calorimeters, and a muon detector.

All criteria used to select candidate $D_s \rightarrow \phi\pi$ decays, with the exception of Čerenkov identification requirements and the ϕ mass cut, were chosen to maximize $S/\sqrt{S+B}$, where S is the number of $D^+ \rightarrow K^-\pi^+\pi^+$ signal events in data, scaled to the level expected for $D_s \rightarrow \phi\pi$, and B is the number of background events from appropriate sideband regions of the $\phi\pi$ mass distribution.

To reconstruct the $D_s \rightarrow \phi\pi$ and $D^+ \rightarrow K^-\pi^+\pi^+$ candidates, three-prong decay vertices with charge of ± 1 were selected. All decay tracks were required to travel through at least one magnet and be of good quality. Decay vertices were required to be located outside the target foils, and the significance of spatial separation from the primary vertex in the beam direction, $\Delta z/\sigma_{\Delta z}$, where $\sigma_{\Delta z}$ is the error on the separation, was required to be at least 11. The component of the D momentum perpendicular to the line joining the primary and secondary vertices was required to be less than $0.35 \text{ GeV}/c$. The transverse impact parameter of the D momentum with respect to the primary vertex was required to be less than $55 \mu\text{m}$. Decay tracks were required to pass closer to the secondary vertex than to the primary vertex, and the sum of the squares of their momenta perpendicular to the D direction was required to be larger than $0.3 (\text{GeV}/c)^2$. The candidates in the decay mode $\phi\pi$ with $\phi \rightarrow K^+K^-$ were also required to have $M(K^+K^-)$ within $\pm 10 \text{ MeV}/c^2$ of the ϕ mass.

For the decay $D^+ \rightarrow K^-\pi^+\pi^+$, the kaon was identified on the basis of charge alone and no Čerenkov identification cuts were needed. For the two same-sign tracks in the decay $D_s \rightarrow \phi\pi$, the track with the highest Čerenkov probability was assumed to be the kaon and the other track the pion. No further Čerenkov identification cuts were applied, given the ϕ mass selection criteria.

The longitudinal and transverse position resolutions for the primary vertex were $350 \mu\text{m}$ and $6 \mu\text{m}$, respectively. The mean momentum of selected D^+ and D_s mesons was $70 \text{ GeV}/c$. For the decay vertices of these mesons, the transverse resolution was about $9 \mu\text{m}$, nearly independent of the momentum, and the longitudinal resolution was about $360 \mu\text{m}$ at $70 \text{ GeV}/c$ and worsened by $30 \mu\text{m}$ for every $10 \text{ GeV}/c$ increase in momentum.

To eliminate any possible background due to reflections from $D^+ \rightarrow K^-\pi^+\pi^+$ with a pion misidentified as a kaon, which appear under and near the D_s signal in the $\phi\pi$ mass plot, we excluded all $\phi\pi$ candidate events with $M(K^-\pi^+\pi^+)$ within $\pm 30 \text{ MeV}/c^2$ of the D^+ mass. The mass distributions for all $\phi\pi$ candidates that survived our selection criteria are shown in Fig. 1. The higher mass peak corresponds to $D_s \rightarrow \phi\pi$ while the lower peak corresponds to the singly Cabibbo-suppressed (SCS) decay $D^+ \rightarrow \phi\pi^+$. The $\phi\pi$ mass distribution before $D^+ \rightarrow K^-\pi^+\pi^+$ background subtraction is shown in Fig. 1(a), with candidates consistent with $D^+ \rightarrow K^-\pi^+\pi^+$ background shown as the hatched region. The $\phi\pi$ mass distribution after the reflection subtraction is shown in Fig. 1(b). The hatched region in Fig. 1(a) appears to be due to a small D_s signal and a linear background that turns on around $1.95 \text{ GeV}/c^2$. The background in Fig. 1(b) is therefore modeled as a piecewise linear function with a discontinuity fixed at $1.95 \text{ GeV}/c^2$. We have studied the sensitivity of our measured lifetime to the position of this discontinuity and have found very little effect. We have included a small systematic error in our total error to account for the change in lifetime when the location of this discontinuity is

varied from 1.95 to 1.99 GeV/ c^2 .

To extract the D_s lifetime we performed a simultaneous unbinned maximum-likelihood fit to the distribution of mass and reduced proper decay time (t^R) of all $\phi\pi$ candidates that pass the selection criteria. The t^R is defined as

$$t^R = (L - L_{min})/c\beta\gamma,$$

where L is the distance between the secondary and primary vertices, and L_{min} is the minimum L value allowed by the cut on the separation between the secondary and primary vertices for this event. We fit events in the ranges $1.75 < M(\phi\pi) < 2.05$ GeV/ c^2 and $0.0 < t^R < 4.0$ ps. From the fit we also measure the lifetime of the SCS decay $D^+ \rightarrow \phi\pi^+$.

The overall likelihood function is

$$\mathcal{L} = \frac{e^{-(N_{pred}-N_{obs})^2/2N_{pred}}}{\sqrt{2\pi N_{pred}}} \prod_i \mathcal{L}_i,$$

with $N_{pred} = N_{D^+} + N_{D_s} + N_{BG}$, where N_{D^+} , N_{D_s} , and N_{BG} are the fitted number of $D^+ \rightarrow \phi\pi^+$, $D_s \rightarrow \phi\pi$, and $\phi\pi$ background events, respectively.

The likelihood for each candidate is

$$\mathcal{L}_i = S_{D^+}(m_i, t_i^R) + S_{D_s}(m_i, t_i^R) + B(m_i, t_i^R)$$

where

$$S_{D^+}(m_i, t_i^R) = F_{D^+} \times \frac{1}{\sqrt{2\pi}\sigma_{D^+}} e^{-(m_{D^+}-m_i)^2/2\sigma_{D^+}^2} \\ \times R_{D^+} \cdot f_{D^+}(t_i^R) \cdot e^{-t_i^R/\tau_{D^+}},$$

$$S_{D_s}(m_i, t_i^R) = F_{D_s} \times \frac{1}{\sqrt{2\pi}\sigma_{D_s}} e^{-(m_{D_s}-m_i)^2/2\sigma_{D_s}^2} \\ \times R_{D_s} \cdot f_{D_s}(t_i^R) \cdot e^{-t_i^R/\tau_{D_s}},$$

$$B(m_i, t_i^R) = F_{BG} \times R_{BG} \cdot (e^{-t_i^R/\tau_{BG1}} + C e^{-t_i^R/\tau_{BG2}}) \\ \times \begin{cases} A_1 + S_1 m_i & (\text{for } m_i < m_0) \\ A_2 + S_2 m_i & (\text{for } m_i \geq m_0) \end{cases}.$$

The functions $S_{D^+}(m_i, t_i^R)$, $S_{D_s}(m_i, t_i^R)$, and $B(m_i, t_i^R)$ are the likelihood functions for $D^+ \rightarrow \phi\pi^+$, $D_s \rightarrow \phi\pi$, and $\phi\pi$ background, respectively. The coefficients F_{D^+} , F_{D_s} , and F_{BG} are the ratios of the D^+ , D_s , and the background, to the total number of events: $F_{D^+} = N_{D^+}/N_{pred}$, $F_{D_s} = N_{D_s}/N_{pred}$, and $F_{BG} = N_{BG}/N_{pred}$. m_i and t_i^R are the mass and the reduced proper decay time of the $\phi\pi$ candidates. σ_{D^+} and σ_{D_s} are the D^+ and D_s mass resolutions. τ_{D^+} and τ_{D_s} are the D^+ and D_s lifetimes. The background in the mass distribution is described as two linear functions with slopes S_1 and S_2 which are determined from the fit, and m_0 is the position of the discontinuity in the background mass shape, which is fixed. The terms A_1 and A_2 are obtained from the normalization and the size of the discontinuity, which is determined from the fit. The coefficients R_{D^+} , R_{D_s} , and R_{BG} are the normalizations of the fit functions over t^R in the limits of the fit.

The functions $f_{D^+}(t_i^R)$ and $f_{D_s}(t_i^R)$ are the reconstruction efficiency functions of t^R , for $D^+ \rightarrow \phi\pi^+$ and $D_s \rightarrow \phi\pi$. These efficiency functions are determined from the CF $D^+ \rightarrow K^-\pi^+\pi^+$ decay in data, and from the ratios of MC efficiencies for the SCS $D^+ \rightarrow \phi\pi^+$ decay and the $D_s \rightarrow \phi\pi$ decay, separately, to that for $D^+ \rightarrow K^-\pi^+\pi^+$ decay, as follows:

$$f_{D^+}(t_i^R) = \epsilon_{D^+ \rightarrow K\pi\pi}^{Data}(t_i^R) \times \frac{\epsilon_{D^+ \rightarrow \phi\pi}^{MC}(t_i^R)}{\epsilon_{D^+ \rightarrow K\pi\pi}^{MC}(t_i^R)},$$

$$f_{D_s}(t_i^R) = \epsilon_{D^+ \rightarrow K\pi\pi}^{Data}(t_i^R) \times \frac{\epsilon_{D_s \rightarrow \phi\pi}^{MC}(t_i^R)}{\epsilon_{D^+ \rightarrow K\pi\pi}^{MC}(t_i^R)}.$$

We determine the efficiency for $D^+ \rightarrow K^-\pi^+\pi^+$ from data by comparing the background subtracted t^R distribution for $D^+ \rightarrow K^-\pi^+\pi^+$ to an exponential function with the world average D^+ lifetime [1], $\tau(D^+) = 1.057 \pm 0.015$ ps. The uncertainty on the D^+ lifetime contributes to our systematic error.

We prefer to determine the functions $f_D(t_i^R)$, $f_{D^+}(t_i^R)$ and $f_{D_s}(t_i^R)$, from data and the ratios of efficiencies from MC to reduce our dependency on MC. Most uncertainties that arise from MC simulation should cancel in the ratios and, as a systematic check, we also measure the D_s lifetime using the functions $f_{D^+}(t_i^R)$ and $f_{D_s}(t_i^R)$ derived only from MC. We use the same cuts for the $\phi\pi$ and $K^-\pi^+\pi^+$ data samples in order to minimize any bias in the efficiency ratios due to the selection criteria.

The background in the t^R distribution is parameterized as a sum of two exponential functions with lifetimes of τ_{BG_1} and τ_{BG_2} , and a relative coefficient C . The parameters were determined from the t^R distribution for the D_s sidebands. As a systematic check they were also allowed to float in the unbinned maximum-likelihood fit, with no significant effect on the measured D_s lifetime; a small systematic error is included in our total error to account for this effect.

The projections of the data and the best fit function from the unbinned maximum-likelihood fit on the $M(\phi\pi)$ and t^R distributions for all events that pass the selection criteria are shown in Figs. 2 and 3(a), respectively. For the subset of events within ± 25 MeV/ c^2 of the D_s mass, the projections of these fit results on the t^R distribution, scaled for the new mass range, are shown in Fig. 3(b). This illustrates that our fit describes the data well for events in a narrow window around the D_s signal where the background is small. The fit yields 1662 ± 56 $D_s \rightarrow \phi\pi$ signal events with a D_s lifetime $\tau(D_s) = 0.518 \pm 0.014$ ps, and 997 ± 39 $D^+ \rightarrow \phi\pi^+$ signal events with a D^+ lifetime $\tau(D^+) = 1.065 \pm 0.048$ ps. The D^+ lifetime is in good agreement with current D^+ lifetime measurements, indicating that the MC models the relative efficiency of $\phi\pi$ to $K^-\pi^+\pi^+$ well. The projections from the fit on the t^R distribution for $D^+ \rightarrow \phi\pi^+$ and $D_s \rightarrow \phi\pi$ are not pure exponentials because of the nonuniform detector efficiencies, which were parameterized by the functions $f_{D^+}(t_i^R)$ and $f_{D_s}(t_i^R)$ as described above.

Since ratios of MC efficiencies are used in the fit, most systematic errors cancel in the final D_s lifetime measurement. However, some uncertainties remain. The sources of these are summarized in Table 2, and quantitative estimates of the errors are listed. In general, the estimates come from re-fitting after varying data selection criteria, parameters, and mass or t^R regions used. The total systematic error comes from adding the contributions in quadrature.

Other checks were performed such as fitting to only a portion of the t^R range, which would check our efficiency functions across the t^R range considered, and measuring the lifetime of the D_s^+ and D_s^- separately. Variations in results were found to be small compared to the statistical error. Uncertainties due to target absorption and scattering of charm secondaries are expected to be small due to the thinness of the target foils and the requirement that decay vertices be located outside the target foils. In addition, since we use the $D^+ \rightarrow K^-\pi^+\pi^+$ data to correct for efficiency, any such effects should be accounted for.

Finally, as a test of our fitting procedure, we fitted our $K^-\pi^+\pi^+$ data to measure the D^+ lifetime using an unbinned maximum-likelihood fit similar to that used to fit the $\phi\pi$ data. The efficiency function for the $D^+ \rightarrow K^-\pi^+\pi^+$ was determined only from MC. The fit yielded 62651 ± 337 D^+ signal events, shown in Ref. [7], with a measured D^+ lifetime that agrees with the world average value [1] to better than the 1.5% error on the world average value.

In conclusion, we have made a new precise measurement of the D_s lifetime using 1662 ± 56 fully reconstructed $D_s \rightarrow \phi\pi$ decays. The D_s lifetime is measured using an unbinned maximum-likelihood fit to be $0.518 \pm 0.014 \pm 0.007$ ps. This value is about two standard deviations higher than the present world average of 0.467 ± 0.017 ps [1]. Using our result and the world average D^0 lifetime [1],

we find the ratio of our D_s lifetime to the D^0 lifetime to be

$$\frac{\tau(D_s)}{\tau(D^0)} = 1.25 \pm 0.04 \quad (6\sigma \text{ difference from unity})$$

showing significantly different lifetimes for the D_s and D^0 . This result may be used to constrain the contributions of various decay mechanisms to charm decay and further refine our quantitative understanding of the hierarchy of charm particle lifetimes.

We gratefully acknowledge the assistance of the staffs of Fermilab and of all the participating institutions. This research was supported by the Brazilian Conselho Nacional de Desenvolvimento Científico e Tecnológico, CONACyT (Mexico), the Israeli Academy of Sciences and Humanities, the U.S. Department of Energy, the U.S.-Israel Binational Science Foundation and the U.S. National Science Foundation. Fermilab is operated by the Universities Research Association, Inc., under contract with the United States Department of Energy.

References

- [1] Particle Data Group, C. Caso *et al.*, Eur. Phys. J. C 3 (1998) 1.
- [2] S. E. Csorna *et al.*, Phys. Lett. B 191 (1987) 318; H. Albrecht *et al.*, Phys. Lett. B 210 (1988) 267; J. R. Raab *et al.*, Phys. Rev. D 37 (1988) 2391; M. P. Alvarez *et al.*, Z. Phys. C 47 (1990) 539; S. Barlag *et al.*, Z. Phys. C 46 (1990) 563; P. L. Frabetti *et al.*, Phys. Rev. Lett. 71 (1993) 827.
- [3] R. J. Morrison and M. S. Witherell, Ann. Rev. Nucl. Part. Sci. 39 (1989) 183; T. E. Browder, K. Honscheid, and D. Pedrini, Ann. Rev. Nucl. Part. Sci. 46 (1996) 395; G. Bellini, I. Bigi, and P. J. Dornan, Phys. Rept. 289 (1997) 1.
- [4] I. I. Bigi and N. G. Uraltsev, Z. Phys. C 62 (1994) 623.
- [5] E. M. Aitala *et al.*, submitted to Phys. Rev. D, FERMILAB-PUB/98-297-E and hep-ex/9809029 (1998).
- [6] D. Bartlett *et al.*, Nucl. Instrum. Methods Phys. Res., Sect. A 260 (1987) 55.
- [7] E. M. Aitala *et al.*, Phys. Lett. B 403 (1997) 377.

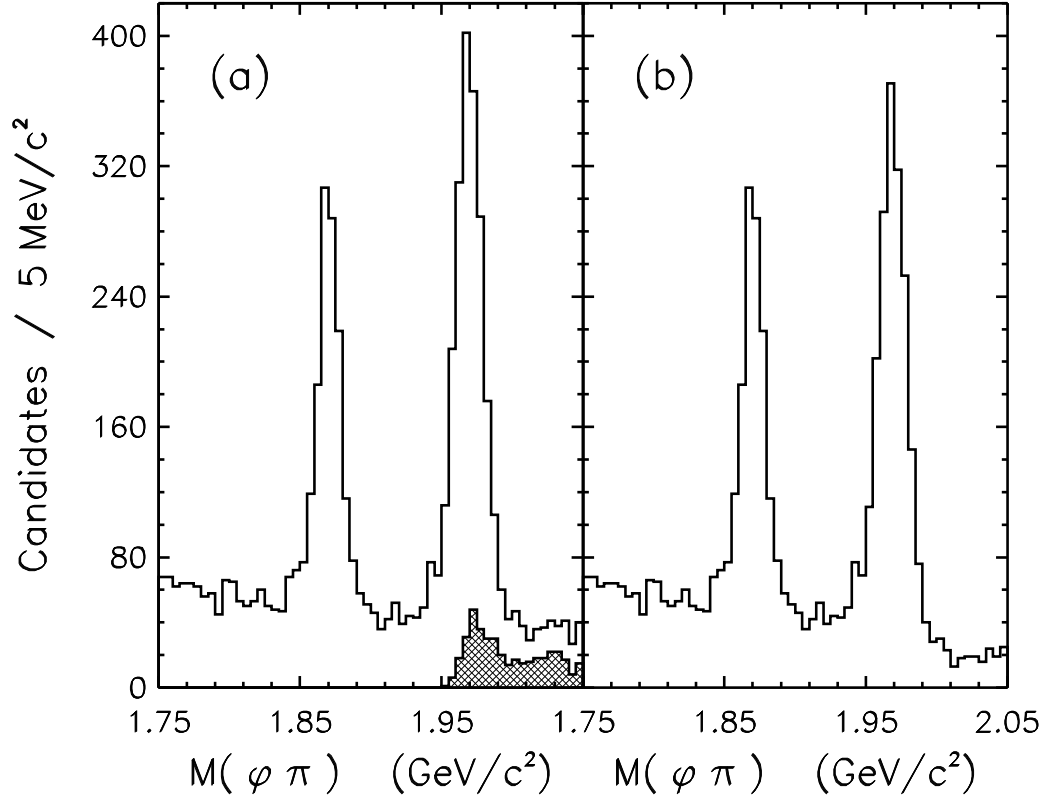


Fig. 1. The $\phi\pi$ mass distributions: (a) before excluding candidates with $M(K^-\pi^+\pi^+)$ within $\pm 30 \text{ MeV}/c^2$ of the D^+ mass, which are shown as the hatched histogram; (b) after excluding candidates with $M(K^-\pi^+\pi^+)$ within $\pm 30 \text{ MeV}/c^2$ of the D^+ mass, as described in the text.

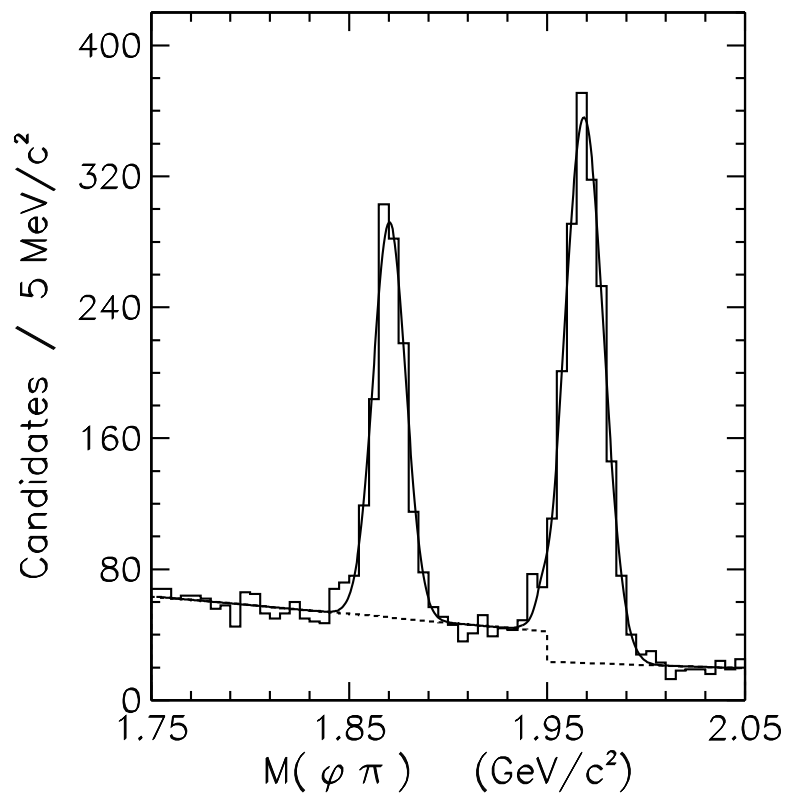


Fig. 2. The projection from the unbinned maximum-likelihood fit on the $M(\phi\pi)$ distribution, with the discontinuity in the linear background fixed at $1.95 \text{ GeV}/c^2$. The two peaks are the SCS D^+ signal with a fitted yield of 997 ± 39 events, and the D_s signal with a fitted yield of 1662 ± 56 events, as described in the text.

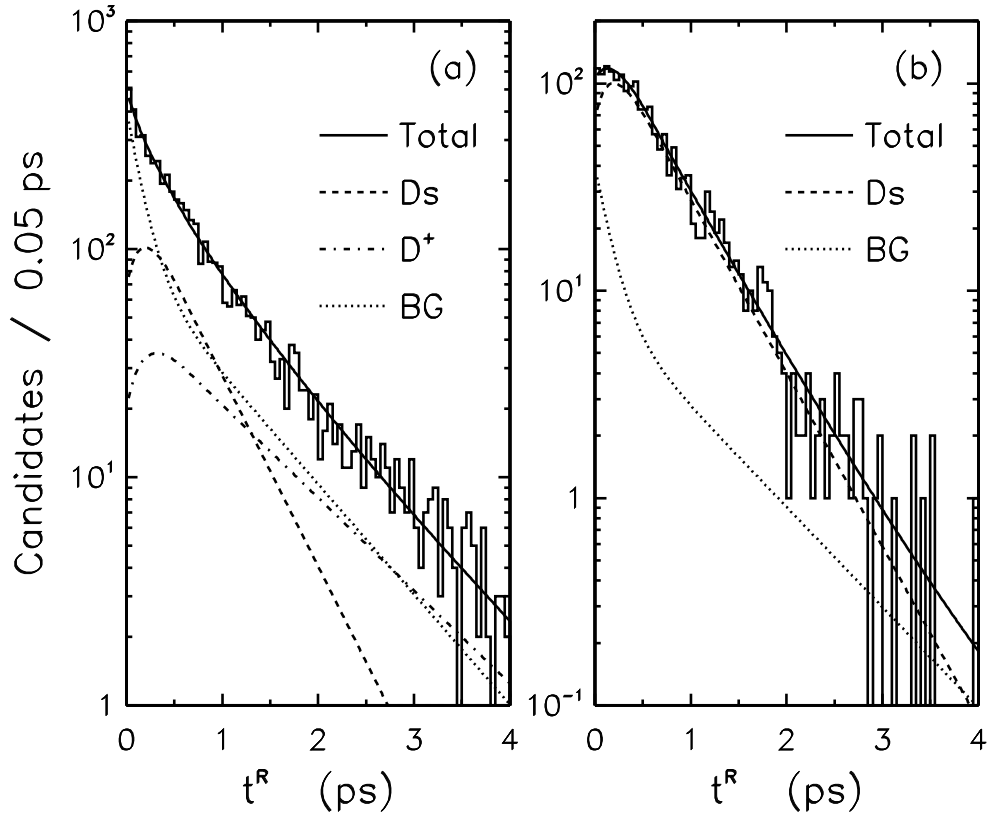


Fig. 3. The projection of the data and the best fit function from the unbinned maximum-likelihood fit, on the reduced proper decay time distribution. (a) All events that pass the selection criteria (histogram). Also shown are the total fit function (solid curve), and the contribution to the fit from $D_s \rightarrow \phi\pi$ (dashed curve), $D^+ \rightarrow \phi\pi^+$ (dashed-dotted curve), and $\phi\pi$ background (dotted curve). (b) Events within $\pm 25 \text{ MeV}/c^2$ of the D_s mass (histogram). Also shown are the total fit function (solid curve), and the contribution to the fit from $D_s \rightarrow \phi\pi$ (dashed curve) and from $\phi\pi$ background (dotted curve), as described in the text.

Table 1

Summary of the phase space (PS) factors, in arbitrary units, and the phase space ratios, for 2, 3, 4, and 5-body decay modes of the D^0 and D_s . The phase space factors are calculated for the final states shown, with no intermediate resonances.

D^0		D_s		PS(D^0)/PS(D_s)
Decay Mode	PS	Decay Mode	PS	
$K^-\pi^+$	1.45	$K^+\bar{K}^0$	1.36	1.07
$K^-\pi^+\pi^0$	1.70	$K^+K^-\pi^+$	1.32	1.29
$K^-\pi^+\pi^+\pi^-$	0.537	$K^0K^-\pi^+\pi^+$	0.247	2.17
$\bar{K}^0\pi^+\pi^+\pi^-\pi^-$	0.0548	$K^+K^-\pi^+\pi^+\pi^-$	0.0127	4.31

Table 2

Summary of the systematic uncertainties assigned to the D_s lifetime, as described in the text.

Source of Uncertainty	Systematic Error
D^+ lifetime uncertainty [1]	0.004 ps
Size of $D^+ \rightarrow K^-\pi^+\pi^+$ reflection	0.003 ps
Data selection criteria	0.003 ps
Likelihood efficiency functions, $f_D(t_i^R)$	0.003 ps
t^R parameterization of background	0.002 ps
Position of step in background function	0.002 ps
Monte Carlo production model	0.002 ps
Total systematic error	0.007 ps